Structure and Magnetic Properties of a Mixed-Valence Heptanuclear Manganese Cluster†

Gian Luca Abbati,‡ Andrea Cornia,‡ Antonio C. Fabretti,‡ Andrea Caneschi,§ and Dante Gatteschi*,§

Departments of Chemistry, University of Modena, via G. Campi 183, 41100 Modena, Italy, and University of Florence, via Maragliano 75, 50144 Florence, Italy

Received January 2, 1998

Two novel polynuclear manganese(II,III) complexes have been synthesized by exploiting controlled methanolysis. A one-pot reaction of $MnCl_2$, NaOMe, dibenzoylmethane (Hdbm), and O_2 in anhydrous methanol, followed by recrystallization from MeOH/$CHCl_3$ mixtures, afforded the alkoxomanganese complexes $[Mn_7(OMe)_{12}(dbm)_6]\cdot CHCl_3\cdot 14MeOH$ (**2**) and $[Mn_2(OMe)_2(dbm)_4]$ (**3**). Complex **2** crystallizes in trigonal space group $R\bar{3}$ with $a = 14.439(2)$ Å, $\alpha = 86.34(1)°$, and $Z = 1$. Complex **3** crystallizes in triclinic space group $P\bar{1}$ with $a = 9.612(1)$ Å, $b = 10.740(1)$ Å, $c = 13.168(1)$ Å, $\alpha = 80.39(1)°$, $\beta = 87.66(1)°$, $\gamma = 83.57(1)°$, and $Z = 1$. The solid-state structure of **2** comprises a $[Mn_6(OMe)_{12}(dbm)_6]$ "crown" with crystallographically imposed 6-fold symmetry plus a central manganese ion. The layered Mn/O core mimics a fragment of the manganese oxide mineral lithiophorite. Conductivity measurements confirmed the nonionic character of **2** and suggested a mixed-valence $Mn^{II}_3Mn^{III}_4$ formulation. The metrical parameters of the core were analyzed with the aid of bond-valence sum calculations. The central ion is essentially a valence-trapped Mn^{II} ion, whereas the average Mn−O distances for the manganese ions of the "crown" are consistent with the presence of two Mn^{II} and four Mn^{III} ions. However, ^1H NMR spectra in solution strongly support valence localization and suggest that the observed solid-state structure may be a result of static disorder effects. Magnetic susceptibility vs *T* and magnetization vs field data at low temperature are consistent with an $S = {}^{17}/_2$ ground state. Complex **3** is a symmetric alkoxo-bridged dimer. The two high-spin Mn^{III} ions are antiferromagnetically coupled with $J = 0.28(4)$ cm^{-1}, $g = 1.983(2)$, and $D = -2.5(4)$ cm^{-1}.

Introduction

Polynuclear manganese complexes are attracting considerable attention in several different fields ranging from bioinorganic chemistry to solid-state physics.[1] Low-nuclearity species have been extensively studied as models for the water oxidizing complex in photosystem II,[2] whereas nanometer-size clusters with high-spin ground states are currently being investigated as single-molecule magnets.[3] From a synthetic point of view, chemists have learned to exploit hydrolytic reactions which naturally lead to insoluble metal oxides and oxohydroxides as final products. By proper use of suitable organic ligands, mainly carboxylates,[4] polyamines,[5] and polyols,[6] the "growth" of the metal cores can be controlled in such a way to obtain finite-size clusters. Alkoxide ligands represent an alternative, powerful tool for assembling metal clusters,[7−11] as demonstrated by recent work on alkoxoiron(III) complexes,[8,9a−c,10] whose metal/

* To whom correspondence should be addressed. E-mail: gattesch@blu.chim1.unifi.it. Tel.: +39-55-3216326. Fax: +39-55-354845.

† Dedicated to Prof. Achim Müller in the occasion of his 60th birthday.

‡ University of Modena.

§ University of Florence.

(1) (a) Caneschi, A.; Gatteschi, D.; Sessoli, R. *J. Chem. Soc., Dalton Trans.* **1997**, 3963. (b) Villain, J.; Hartman-Boutron, F.; Sessoli, R.; Rettori, A. *Europhys. Lett*. **1994**, *27*, 159. (c) Politi, P.; Rettori, A.; Hartmann-Boutron, F.; Villain, J. *Phys. Rev. Lett*. **1995**, *75*, 537. (d) Hennion, M.; Pardi, L.; Mirebeau, L.; Suard, E.; Sessoli, R.; Gatteschi, D. *Phys. Rev*. **1997**, *B56*, 8819.

(2) (a) Wieghardt, K. *Angew. Chem., Int. Ed. Engl*. **1994**, *33*, 725. (b) Debus, R. J. *Biochem. Biophys. Acta* **1992**, *1102*, 269. (c) Brudvig, G. W.; Thorp, H. H.; Crabtree, R. H. *Acc. Chem. Res.* **1991**, *24*, 311. (d) Christou, G. *Acc. Chem. Res.* **1989**, *22*, 328.

(3) (a) Ballou, R.; Barbara, B.; Lionti, F.; Gatteschi, D.; Sessoli, R. *Nature* **1996**, *383*, 145. (b) Friedman, J.; Maciejewski, J.; Sarachik, M. P.; Tejada, J.; Ziolo, R. *Phys. Rev. Lett.* **1996**, *76*, 3820. (c) Caneschi, A.; Gatteschi, D.; Pardi, L.; Sessoli, R. *Science* **1994**, *265*, 1054. (d) Aubin, S. M. J.; Sun, Z.; Guzei, I. A.; Rheingold, A. L.; Christou, G.; Hendrickson, D. N. *J. Chem. Soc., Chem. Commun.* **1997**, 2239.

(4) (a) Squire, R. C.; Aubin, S.; Folting, K.; Streib, W.; Hendrickson, D. N.; Christou, G. *Inorg. Chem*. **1995**, *34*, 6463. (b) Gorun, S. M.; Stibrany, R. T. U.S. Patent 5,041,575, 1991. (c) Lis, T. *Acta Crystallogr*. **1980**, *B36*, 2042. (d) Boyd, P.; Li, Q.; Vincent J. B.; Folting, K.; Chang, H.-R.; Strieb, W.; Huffman, J. C.; Christou, G.; Hendrickson, D. N. *J. Am. Chem. Soc*. **1988**, *110*, 8537. (e) Sessoli, R.; Tsai, H.; Schake, A.; Wang, S.; Vincent, J.; Folting, K.; Gatteschi, D.; Hendrickson, D. N.; Christou, G. *J. Am. Chem. Soc*. **1993**, *115*, 1804. (f) Eppley, H.; Tsai, H.; de Vries, N.; Folting, K.; Christou, G.; Hendrickson, D. N. *J. Am. Chem. Soc*. **1995**, *117*, 301. (g) Tsai, H.; Wang, S.; Folting, K.; Streib, W.; Hendrickson, D. N.; Christou, G. *J. Am. Chem. Soc*. **1995**, *117*, 2503. (h) Low, D. W.; Eichhorn, D. E.; Dragonescu, A.; Armstrong, W. H. *Inorg. Chem.* **1991**, *30*, 87. (i) Christmas, C.; Vincent, J.; Chang, H.; Huffman, J.; Christou, G.; Hendrickson, D. N. *J. Am. Chem. Soc*. **1988**, *110*, 823. (j) Blackman, A.; Huffman, J. C.; Lobkovsky, E.; Christou, C. *Polyhedron* **1992**, *11*, 251. (k) Baike, A.; Howes, A.; Hursthouse, M.; Quick, A.; Thornton, P. *J. Chem. Soc., Chem. Commun.* **1986**, 1587. (l) Lis, T.; Jezowska-Trzebiatowska, B. *Acta Crystallogr.* **1977**, *B33*, 2112. (m) Libby, E.; Folting, K.; Huffman, C. J.; Christou, G. *Inorg. Chem*. **1993**, *32*, 2549. (n) Wang, S.; Huffman, J. C.; Folting, K.; Streib, W.; Lobkovsky, E.; Christou, G. *Angew. Chem., Int. Ed. Engl*. **1991**, *30*, 1672.

(5) (a) Bhula R.; Weatherburn, D. C. *Angew. Chem., Int. Ed. Engl*. **1991**, *30*, 688. (b) Grillo, V.; Knapp, M.; Bollinger, J.; Hendrickson, D. N.; Christou, G. *Angew. Chem., Int. Ed. Engl*. **1996**, *35*, 1818. (c) Hagen, K. S.; Armstrong, W. H.; Olmstead, M. *J. Am. Chem. Soc*. **1989**, *111*, 774. (d) Wieghardt, K.; Bossek, U.; Gebert, W. *Angew. Chem., Int. Ed. Engl*. **1983**, *22*, 328. (e) Bhula, R.; Collier, S.; Robinsin, W.; Weatherburn, D. C. *Inorg. Chem.* **1990**, *29*, 4027.

(6) (a) Cavalluzzo, M.; Chen Q.; Zubieta, J. *J. Chem. Soc., Chem. Commun.* **1993**, 191. (b) Goldberg, D. P.; Caneschi, A.; Delfs, C. D.; Sessoli, R.; Lippard, S. J. *J. Am. Chem. Soc*. **1995**, *117*, 5789. (c) Xia, X.; Verelst, M.; Daran, J.-C.; Tuchagues, J.-P. *J. Chem. Soc., Chem. Commun.* **1995**, 2155.

S0020-1669(98)00002-0 CCC: $15.00
Published on Web 07/10/1998

oxygen cores often exhibit closest-packing layered structures which are typical of bulk metal oxides. Surprisingly, manganese chemistry with alkoxide ligands remains a quite unexplored area. Recently, the synthesis of Mn^{II} complexes with cuboidal $[Mn_4(OR)_4]^{4+}$ cores, namely $[Mn_4(OMe)_4(L)_4(MeOH)_4]$ (HL = Hdbm, Hdpm) and $[Mn_4(OEt)_4(dpm)_4(EtOH)_2]$,[11,12] has been reported. Their extreme sensitivity to air oxidation has been ascribed to the hard-donor character of alkoxide ligands, which stabilize high-valent metal states.[11] We therefore investigated the possibility of exploiting this tendency to address the synthesis of high-nuclearity, preferably high-valent manganese clusters which may behave as single-molecule magnets.[3] The synthesis, solid-state structure, and magnetic properties of the complex $[NaMn^{III}_6(OMe)_{12}(dbm)_6]BPh_4 \cdot x CHCl_3$ (**1**) have been already reported.[12,13] The cluster comprises a ring of six Mn^{III} ions, with a sodium ion in the center. The coupling between the Jahn−Teller distorted ions is ferromagnetic, yielding a ground $S = 12$ state. Substitution of the sodium ion with a magnetic ion appeared to be exciting for tuning the magnetic properties of the clusters and also for introducing valence fluctuation, exploring the possibility of synthesizing either trapped or delocalized mixed-valence species. We report here the synthesis and characterization of the novel heptanuclear alkoxomanganese cluster $[Mn_7(OMe)_{12}(dbm)_6] \cdot CHCl_3 \cdot 14MeOH$ (**2**), which has noninteger average valence of the manganese ions. It is a high-spin molecule whose layered structure mimics a fragment of the manganese oxide mineral lithiophorite. We report also the structure and solid-state magnetic behavior of the dimeric complex $[Mn^{III}_2(OMe)_2(dbm)_4]$ (**3**), which was obtained as a byproduct of the synthetic procedure used for **2**.

Experimental Section

Analytical Procedures. ^{1}H NMR spectra were recorded on a Bruker Advance DPX spectrometer operating at 200 MHz. IR and UV−vis spectra were recorded on FTIR Bruker IFS 113v and Perkin-Elmer Lambda 9 spectrometers. Conductivity measurements were carried out by using an Amel 134 conductometer. C, H, N elemental analyses were performed using a Carlo Erba 1106 automatic analyzer. Mn was determined by an ICP (inductively coupled plasma) spectrometer, SPECTRO D, after decomposition of the sample in a Kjeldahl flask by treatment with sulfuric acid.[14] Major calculations were performed on an Alpha 3000/800S computer and an RISC workstation.

Synthesis. All procedures were performed under aerobic conditions with strict exclusion of moisture. All reagents and solvents were used as received, with exception of methanol, which was distilled over $Mg(OMe)_2$ shortly before use.[15] The complex $Mn(dbm)_3$ (**4**) was synthesized by a literature procedure.[16b]

$[Mn_7(OMe)_{12}(dbm)_6] \cdot CHCl_3 \cdot 14MeOH$ (2). To 10 mmol of $MnCl_2$ dissolved in 30 mL of anhydrous methanol was added dropwise with vigorous stirring a solution containing 40 mmol of NaOMe and 10 mmol of Hdbm in 120 mL of anhydrous methanol, yielding a brown precipitate which was rapidly collected by filtration and dried under vacuum. A 0.25-g amount of freshly prepared precipitate was dissolved in chloroform (10 mL) and the resulting solution was layered with a double volume of anhydrous methanol in a sealed tube. Dark-brown cubes of **2** formed in 1−2 weeks. The overall yield was about 53% (referred to Mn). The crystals underwent extremely rapid solvent loss when removed from their mother liquid and immediately became a brown microcrystalline powder. Analyses were performed on crystals washed with an MeOH−$CHCl_3$ 1:1 (v/v) mixture and dried under vacuum. Anal. Calcd for $[Mn_7(OMe)_{12}(dbm)_6]$: C, 58.44; H, 4.90; Mn, 18.43. Found: C, 58.04; H, 4.94; Mn, 18.92. UV−vis (solid): 10 000, 17 000, 21 000 cm^{-1}. IR (KBr pellets): 3430 (s), 3060 (m), 2918 (m), 2811 (m), 1618 (m), 1605 (s), 1555 (s), 1520 (s), 1480 (s), 1453 (s), 1442 (m), 1390 (s), 1308 (s), 1290 (s), 1226 (s), 1182 (m), 1096 (w), 1069 (s), 1060 (s), 1023 (s), 1000 (w), 940 (w), 756 (m), 720 (s), 688(s), 624 (s), 551 (s) cm^{-1}.

$[Mn_2(OMe)_2(dbm)_4]$ (3). Air-stable dark-brown crystals of **3** were obtained in a manner analogous to that for **2**, replacing the layering of liquid methanol with slow diffusion of methanol vapors to induce crystallization. Anal. Calcd for **3**: C, 69.93; H, 4.73. Found on a vacuum-dried sample: C, 69.83; H, 4.76. UV−vis (solid): 9000, 18 000, 21 000 cm^{-1}. IR (KBr pellets): 1594 (s), 1509 (s), 1476 (s), 1453 (m), 1441 (m), 1388 (s), 1341 (m), 1306 (s), 1285 (s), 1220 (m), 1173 (m), 1121 (w), 1050 (m), 1015 (m), 988 (m), 925 (m), 764 (w), 726 (s), 688 (s), 623 (m), 570 (w), 514 (w) cm^{-1}.

$[Mn(dbm)_2(H_2O)_2]$ (6). A variation of the method of Fernelius and Bryant was used.[17] Under a dinitrogen atmosphere, 4 mmol of solid $MnBr_2 \cdot 4H_2O$ was quickly added to a solution of Hdbm (8 mmol) and triethylamine (20 mmol) in 40 mL of dioxygen-free MeCN. Upon stirring, a yellow precipitate formed in good yield (about 70%) in few minutes. The mixture was stirred for an additional 30 min; then the precipitate was collected by filtration and dried under a dinitrogen stream. Compound **6** underwent extremely rapid air oxidation if wet or if in solution. The dry material was air-stable. Anal. Calcd for **6**: C, 67.04; H, 4.88. Found: C, 66.57; H, 4.92.

X-ray Crystallography. X-ray-quality samples of **2** and **3** were obtained directly as described above. Structures were solved using direct methods (SIR92[18]) and refined using the SHELXL-93 package.[19] Details of the crystal data and structure refinement are reported in Table 1. All non-hydrogen atoms, with the exception of solvent atoms, were refined with anisotropic thermal parameters. Unless otherwise stated, hydrogen atoms were treated as fixed contributors in calculated positions and refined isotropically with $B(H) = 1.2B_{eq}(C)$. Final atomic coordinates for **2** and **3** are given in Tables 2 and 3, respectively. Selected interatomic distances and angles can be found in Tables 4 and 5, respectively. CIF files for **2** and **3** are available as Supporting Information.

$[Mn_7(OMe)_{12}(dbm)_6] \cdot CHCl_3 \cdot 14MeOH$ (2). A dark-brown cube (0.38 × 0.72 × 0.66 mm) was removed from the mother liquid and mounted under a cold dinitrogen stream on the top of a quartz glass

(7) (a) Taft, K. L.; Caneschi, A.; Pence, L.; Delfs, C. D.; Papaefthymiou, G. C.; Lippard, S. J. *J. Am. Chem. Soc.* **1993**, *115*, 11753 and references therein. (b) Khan, M. I.; Chen, Q.; Höpe, H.; Parkin, S.; O'Connor, C. J.; Zubieta, J. *Inorg. Chem.* **1993**, *32*, 2929 and references therein.
(8) (a) Caneschi, A.; Cornia, A.; Lippard, S. J. *Angew. Chem., Int. Ed. Engl.* **1995**, *34*, 467. (b) Caneschi, A.; Cornia, A.; Fabretti, A. C.; Foner, S.; Gatteschi, D.; Grandi, R.; Schenetti, L. *Chem. Eur. J.* **1996**, *2*, 1379. (c) Abbati, G. L.; Caneschi, A.; Cornia, A.; Fabretti, A. C.; Gatteschi, D.; Malavasi, W.; Schenetti, L. *Inorg. Chem.* **1997**, *36*, 6443.
(9) (a) Caneschi, A.; Cornia, A.; Fabretti, A. C.; Gatteschi, D.; Malavasi, W. *Inorg. Chem.* **1995**, *34*, 4660. (b) Caneschi, A.; Cornia, A.; Fabretti, A. C.; Gatteschi, D. *Angew. Chem., Int. Ed. Engl.* **1995**, *34*, 2716. (c) Cornia, A.; Gatteschi, D.; Hegetschweiler, K. *Inorg. Chem.* **1994**, *33*, 1559. (d) Taft, K. L.; Papaefthymiou, G. C.; Lippard, S. J. *Inorg. Chem.* **1994**, *33*, 1510. (e) Caneschi, A.; Cornia, A.; Lippard, S. J.; Papaefthymiou, G. C.; Sessoli, R. *Inorg. Chim. Acta* **1996**, *243*, 295.
(10) Le Gall, F.; Fabrizi de Biani, F.; Caneschi, A.; Cinelli, P.; Cornia, A.; Fabretti, A. C.; Gatteschi, D. *Inorg. Chim. Acta* **1997**, *262*, 123.
(11) Caneschi, A.; Pence, L.; Lippard, S. J. *Inorg. Chem.* **1996**, *35*, 3069.
(12) Abbreviations used in the text: Hdbm = dibenzoylmethane; Hdpm = dipivaloylmethane; Hhmp = 2-(hydroxymethyl)pyridine; tren = tris(aminoethyl)amine; Htphpn = *N*,*N*,*N*′,*N*′-tetrakis(2-pyridylmethyl)-2-hydroxypropane-1,3-diamine.
(13) Abbati, G. L.; Cornia, A.; Fabretti, A. C.; Caneschi, A.; Gatteschi, D. *Inorg. Chem.* **1998**, *37*, 1430.
(14) Ingram, G. *Methods of Organic Elemental Microanalysis*; Chapman & Hall: London, 1962; p 274.
(15) Vogel, A. I. *Practical Organic Chemistry*, 3rd ed.; Longmans: London, 1959; p 169.
(16) (a) Zaitseva, E. G.; Baidina, I. A.; Stabnikov, P. A.; Borisov, S. V.; Igumenov, I. K. *Zh. Strukt. Khim.* **1990**, *31*, 184. See also *Chem. Abstr.* **1990**, *113*, 88602h. (b) Barra, A.-L.; Gatteschi, D.; Sessoli, R.; Abbati, G. L.; Cornia, A.; Fabretti, A. C.; Uytterhoeven, M. G. *Angew. Chem., Int. Ed. Engl.* **1997**, *36*, 2329.
(17) Fernelius, W. C.; Bryant, B. E. *Inorg. Synth.* **1957**, *5*, 105.
(18) Altomare, A.; Burla, M. C.; Camalli, M.; Cascarano, G.; Giacovazzo, C.; Guagliardi, A.; Polidori, G. *J. Appl. Crystallogr.* **1994**, *27*, 435.
(19) Sheldrick, G. M. *SHELXL-93: Program for Crystal Structure Refinement*; University of Goettingen: Goettingen, Germany, 1993.

Table 1. Crystal Data and Experimental Parameters for **2** and **3**

	2	**3**
empirical formula	$Mn_7C_{117}H_{159}O_{38}Cl_3$	$Mn_2C_{62}H_{50}O_{10}$
fw	2664.4	1064.9
space group (No.)	$R\bar{3}$ (148)	$P\bar{1}$ (2)
a, Å	14.439(2)	9.612(1)
b, Å		10.740(1)
c, Å		13.168(1)
α, deg	86.34(1)	80.39(1)
β, deg		87.66(1)
γ, deg		83.57(1)
V, Å^3	2992.6(7)	1331.5(2)
Z	1	1
T, K	188 (2)	293 (2)
μ, mm^{-1}	0.864	0.534
ρ_{obsd}, g cm^{-3}	1.50(1)	1.33(1)
ρ_{calcd}, g cm^{-3}	1.478	1.328
R1,[a] wR2[b]	0.0579, 0.1879[c]	0.0303, 0.0826[d]

[a] On independent reflections with $I > 2\sigma(I)$; $R1 = \sum||F_o| - |F_c||/\sum|F_o|$. [b] On all data; $wR2 = [\sum w(F_o^2 - F_c^2)^2/\sum w(F_o)^4]^{1/2}$. [c] $w = 1/[\sigma^2(F_o^2) + (0.0504P)^2 + (0.25P)]$ and $P = [\max(F_o^2, 0) + 2F_c^2]/3$. [d] $w = 1/[\sigma^2(F_o^2) + (0.0980P)^2 + (3.65P)]$ and $P = [\max(F_o^2, 0) + 2F_c^2]/3$.

Table 2. Selected Atomic Coordinates ($\times 10^4$) and Equivalent Isotropic Displacement Parameters ($\times 10^3$) for **2** at 188 K[a]

atom	*x*/*a*	*y*/*b*	*z*/*c*	U_{eq},[b] Å^2
Mn1	0	0	10000	30(1)
Mn2	1174(1)	785(1)	8163(1)	33(1)
O1	−264(2)	489(2)	8576(2)	41(1)
O2	583(2)	2025(2)	8534(2)	48(1)
O3	1006(2)	1096(2)	6808(2)	48(1)
O4	2498(2)	1253(2)	7924(2)	49(1)
C1	−703(3)	−2(3)	7903(3)	48(1)
C2	895(4)	2890(3)	8167(3)	66(1)
C3	1535(2)	1512(2)	6199(2)	43(1)
C4	2837(2)	1689(2)	7201(2)	42(1)
C5	2411(2)	1808(3)	6352(2)	46(1)
C6	3745(2)	2115(2)	7316(2)	46(1)
C7	4360(2)	2348(3)	6564(3)	51(1)
C8	5188(3)	2734(3)	6715(4)	62(1)
C9	5403(3)	2917(3)	7594(4)	68(1)
C10	4805(3)	2694(3)	8340(4)	70(1)
C11	3982(3)	2296(3)	8207(3)	57(1)
C12	1138(2)	1711(3)	5274(2)	51(1)
C13	181(3)	1841(4)	5232(3)	65(1)
C14	−216(3)	2074(4)	4387(3)	82(2)
C15	333(4)	2135(5)	3581(3)	96(2)
C16	1264(4)	2008(6)	3616(3)	112(2)
C17	1682(3)	1799(5)	4452(3)	88(2)

[a] Numbers in parentheses are estimated standard deviations in the last significant digit. [b] U_{eq} is defined as one-third of the trace of the orthogonalized $\mathbf{U}_{ij}$ tensor.

capillary with grease (Paratone N, supplied by Exxon). A total of 18 108 reflections in the range $2.8 < 2\theta < 56.6°$ were collected at 188 K on a Siemens SMART-CCD system equipped with graphite-monochromated Mo Kα radiation ($\lambda = 0.71069$ Å) and a low-temperature facility. Refinement of 233 parameters on 4615 independent reflections gave R1 = 0.0579 and wR2 = 0.1879. The largest residual electron density peak and hole in the final ΔF map were 0.527 and −1.074 e Å^{-3}. One $CHCl_3$ molecule (located on the $\bar{3}$ axis) and 14 disordered MeOH molecules per unit cell were located. All hydrogen atoms in the cluster, with the exception of H14 and H16, were located on ΔF maps and refined isotropically.

[Mn_2(OMe)$_2$(dbm)$_4$] (3). Diffraction data were collected at room temperature on a 0.3 × 0.3 × 0.2 mm crystal by using an Enraf-Nonius CAD4 diffractometer equipped with graphite-monochromated Mo Kα radiation ($\lambda = 0.71069$ Å). A total of 4671 reflections were collected in the range $4.3 < 2\theta < 57.9°$. Refinement of 403 parameters on 4475 independent reflections gave R1 = 0.0303 and wR2 = 0.0826. The largest residual electron density peak and hole in the final ΔF map were 0.237 and −0.212 e Å^{-3}.

Table 3. Selected Atomic Coordinates ($\times 10^4$) and Equivalent Isotropic Displacement Parameters ($\times 10^3$) for **3** at 293 K[a]

atom	*x*/*a*	*y*/*b*	*z*/*c*	U_{eq},[b] Å^2
Mn1	5846(1)	3884(1)	5693(1)	38(1)
O1	6039(1)	5585(1)	5151(1)	39(1)
O2	5377(1)	2201(1)	6142(1)	50(1)
O3	7082(1)	3273(1)	4607(1)	45(1)
O4	4826(1)	4362(1)	6932(1)	50(1)
O5	7643(1)	3548(2)	6604(1)	56(1)
C1	17353(2)	6006(2)	4828(2)	59(1)
C2	6091(2)	1156(2)	5985(1)	44(1)
C3	7210(2)	1087(2)	5297(2)	49(1)
C4	7634(2)	2130(2)	4628(1)	43(1)
C5	5144(2)	3992(2)	7869(1)	42(1)
C6	6450(2)	3416(2)	8203(1)	52(1)
C7	7637(2)	3236(2)	7568(1)	45(1)
C8	5600(2)	3(2)	6614(2)	46(1)
C9	5747(2)	−1168(2)	6278(2)	56(1)
C10	5238(3)	−2210(2)	6872(2)	66(1)
C11	4603(3)	−2097(2)	7798(2)	76(1)
C12	4462(3)	−953(2)	8155(2)	86(1)
C13	4946(3)	97(2)	7552(2)	67(1)
C14	8815(2)	1962(2)	3879(1)	47(1)
C15	9663(2)	2920(2)	3604(2)	60(1)
C16	10779(3)	2792(3)	2916(2)	72(1)
C17	11039(3)	1703(3)	2492(2)	72(1)
C18	10195(3)	766(3)	2737(2)	80(1)
C19	9083(3)	869(2)	3438(2)	68(1)
C20	4008(2)	4269(2)	8637(1)	43(1)
C21	4081(2)	3756(2)	9674(2)	59(1)
C22	3025(3)	4063(3)	10359(2)	69(1)
C23	1898(2)	4907(3)	10021(2)	69(1)
C24	1810(2)	5429(2)	8999(2)	69(1)
C25	2850(2)	5103(2)	8303(2)	54(1)
C26	9008(2)	2685(2)	8038(2)	49(1)
C27	10215(2)	2754(3)	7430(2)	69(1)
C28	11507(3)	2277(3)	7834(3)	86(1)
C29	11613(3)	1719(3)	8830(2)	80(1)
C30	10440(3)	1630(3)	9446(2)	84(1)
C31	9140(3)	2105(3)	9053(2)	71(1)

[a] Numbers in parentheses are estimated standard deviations in the last significant digit. [b] U_{eq} is defined as one-third of the trace of the orthogonalized $\mathbf{U}_{ij}$ tensor.

Table 4. Selected Interatomic Distances (Å) and Angles (deg) for **2**[a]

Mn1···Mn2	3.2380(7)	Mn2···Mn2^a	3.243(1)
Mn2···Mn2^b	5.605(1)	Mn2···Mn2^c	6.476(1)
Mn1−O1	2.180(2)	Mn2−O3	2.006(2)
Mn2−O4	2.068(2)	Mn2−O1^e	2.086(2)
Mn2−O1	2.185(2)	Mn2−O2	2.023(3)
Mn2−O2^e	2.023(2)		

Mn2···Mn2^a···Mn2^b	119.56(1)	O1^a−Mn1−O1	81.68(8)
O1^d−Mn1−O1	98.32(8)	O1^c−Mn1−O1	180.00
O3−Mn2−O2^e	93.16(10)	O2−Mn2−O2^e	164.91(11)
O3−Mn2−O4	86.80(9)	O2−Mn2−O4	94.92(10)
O2^e−Mn2−O4	99.22(10)	O3−Mn2−O1^e	171.30(10)
O2−Mn2−O1^e	95.79(9)	O2^e−Mn2−O1^e	78.26(10)
O4−Mn2−O1^e	93.12(9)	O3−Mn2−O1	97.73(9)
O2−Mn2−O1	76.02(9)	O2^e−Mn2−O1	89.46(9)
O4−Mn2−O1	170.00(10)	O1^e−Mn2−O1	83.75(11)
O3−Mn2−O2	92.88(10)	O1^a−Mn1−O1	81.68(8)
O1^b−Mn1−O1	98.32(8)	Mn2−O2−Mn2^a	106.56(10)
Mn2^a−O1−Mn2	98.80(9)	Mn2^a−O1−Mn1	98.71(9)
Mn1−O1−Mn2	95.78(9)		

[a] Superscripts are used for symmetry-equivalent atoms [X^a= S_6^1 (X), X^b= S_6^2 (X), etc.].

Magnetic Measurements. Magnetic studies were performed by using a Métronique Ingéniérie MS03 SQUID magnetometer on 25.81- and 31.15-mg vacuum-treated crystalline samples of **2** and **3**, respec-

Table 5. Selected Interatomic Distances (Å) and Angles (deg) for **3**[a]

Mn1···Mn1′	3.1037(6)	Mn1−O1	1.874(1)
Mn1−O2	1.903(1)	Mn1−O3	1.972(1)
Mn1−O4	1.981(1)	Mn1−O5	2.106(1)
Mn1−O1′	2.136(1)		
O1−Mn1−O4	91.85(5)	O2−Mn1−O4	87.65(6)
O3−Mn1−O4	171.25(5)	O1−Mn1−O2	171.15(5)
O1−Mn1−O5	96.98(6)	O4−Mn1−O5	86.04(5)
O2−Mn1−O5	91.80(6)	O3−Mn1−O5	85.71(5)
O1−Mn1−O3	92.03(5)	O2−Mn1−O3	89.72(5)
O2−Mn1−O1′	92.37(5)	O1−Mn1−O1′	78.79(5)
O3−Mn1−O1′	99.44(5)	O4−Mn1−O1′	89.01(5)
O5−Mn1−O1′	173.39(5)		

[a] Primed atoms are related to unprimed ones by an inversion center.

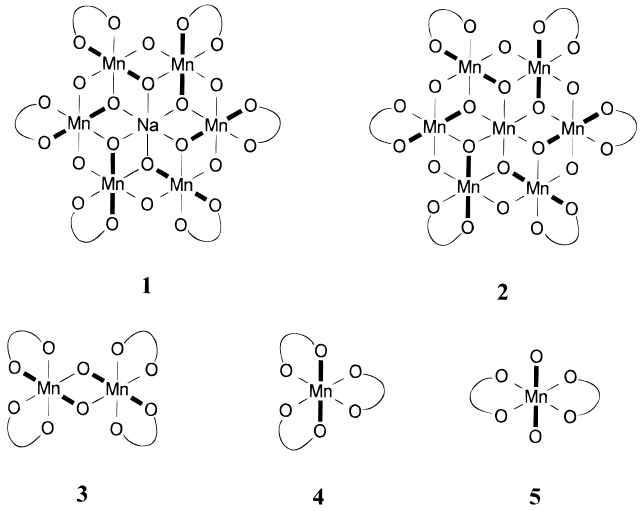

Figure 1. Sketched structures of complexes **1**−**5**. The methyl groups of coordinated methanol in **5** and of methoxide ligands in **1**−**3** are omitted for clarity. Bold lines show the relative orientation of Jahn−Teller elongation axes in the molecules. Solid arcs represent dbm ligands.

tively. A magnetic field of 1 kG for $2.2 < T < 30$ K and 10 kG for $30 < T < 260$ K was applied in χ vs T runs on **2**, whereas a 10-kG magnetic field was used for **3** in the temperature range 2.9−260 K. Magnetization vs field measurements on **2** were performed in the field range 0−70 kG at 2.2 and 4.6 K. A molecular weight corresponding to $[Mn_7(OMe)_{12}(dbm)_6]$ (2096.5) was employed for **2**, consistent with elemental analysis data. Corrections for molecular diamagnetism, estimated from Pascal's constants, were applied throughout.

Results and Discussion

Synthesis and Solid-State Structures. The ability of alkoxide ligands to support condensed structures is well-demonstrated by the growing number of reports on alkoxometal clusters.[7−11] In our approach, we explored the possibility of controlling air oxidation of Mn^{II} salts while promoting aggregation to finite-sized, high-valent manganese clusters. The use of β-diketonates as ancillary ligands followed directly from our previous work on alkoxoiron(III) complexes.[8,9a,b,10] Mononuclear $[Mn(dbm)_3]$ (**4**) and $[Mn(dbm)_2(MeOH)_2]Br$ (**5**)[20] represent the simplest reaction products (Figure 1). The former is invariably obtained from the dissociation of higher-nuclearity species, as found for $Fe(dbm)_3$, and its solid-state structure was recently reinvestigated in conjunction with HF-EPR

(20) Abbati, G. L.; Cornia, A.; Fabretti, A. C.; Giusti, A. Unpublished results.

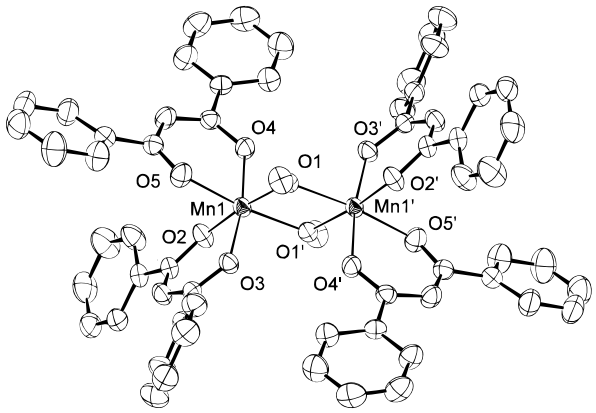

Figure 2. ORTEP view of dimeric compound **3** at 293 K. Thermal ellipsoids are drawn at 50% probability. Hydrogen atoms have been omitted for clarity. Primed atoms are related to unprimed ones by an inversion center.

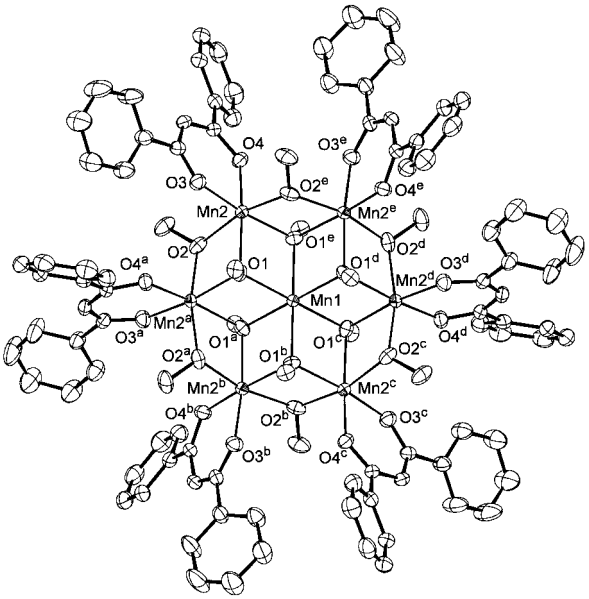

Figure 3. ORTEP view of heptanuclear cluster **2** at 188 K (see the footnote *a* in Table 4). Thermal ellipsoids are drawn at 30% probability. Hydrogen atoms have been omitted for clarity.

experiments.[16b] Dimeric complex **3** (Figure 1) is the simplest polynuclear product obtained by controlled oxidation and aggregation. Its structure closely resembles that of $[Fe_2(OMe)_2(dbm)_4]$ (**7**).[10] The two Mn^{III} ions [Mn···Mn = 3.1037(6) Å] are related by an inversion center and symmetrically bridged by two methoxide ligands (Figure 2). With respect to **7**, the planar $[Mn_2(OMe)_2]$ unit is characterized by markedly different Mn−O bond lengths [Mn1−O1 = 1.874(1) Å, Mn1−O1′ = 2.136(1) Å]. This is a direct consequence of the Jahn−Teller distortion of the coordination polyhedron along the O5−Mn1−O1′ direction. As found in **4**,[16] axial Mn−O bond distances are quite different from each other [Mn1−O1′ = 2.136(1) and Mn1−O5 = 2.106(1) Å]. Furthermore, equatorial Mn−O bonds (average: 1.933 Å) are not equal within experimental errors (see Table 5), although they are similar in couples (Mn1−O3 to Mn1−O4 and Mn1−O1 to Mn1−O2).

The crystal lattice of **2** contains nonionic centrosymmetric $[Mn_7(OMe)_{12}(dbm)_6]$ units (Figure 3) as well as chloroform and methanol molecules. The overall charge of the cluster was determined by comparing molar conductivity values of **2** (Λ_M = 1.14 Ω^{-1} cm^2 mol^{-1} in a $CHCl_3$−MeOH 98−2% v/v mixture; Λ_M = 4.3 Ω^{-1} cm^2 mol^{-1} in acetone) with those of $[NaFe_6$-

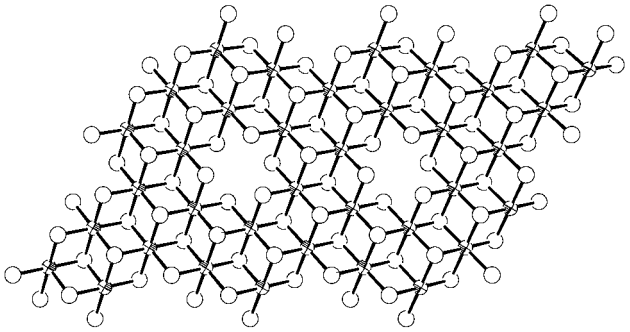

Figure 4. ORTEP view of the Mn/O layer in chalcophanite ($ZnMn_3O_7 \cdot 3H_2O$). Oxygen atoms are depicted as blank spheres; manganese atoms, as crosshatched ones.

$(OMe)_{12}(dbm)_6]X$ ($X = ClO_4$, Cl; $\Lambda_M = 16.3-21.7$ and $100.7-121.6\ \Omega^{-1}\ cm^2\ mol^{-1}$ in the same solvents, respectively[21]). The core of the cluster can be described as an almost planar Mn_6 moiety with a crystallographically imposed S_6 symmetry [deviation from the average plane ± 0.054 Å; $Mn2\cdots Mn2^a = 3.243(1)$ Å; $Mn2\cdots Mn2^a\cdots Mn2^b = 119.56(1)°$] plus a central Mn ion (Table 4). The core is linked by μ_2-OMe and μ_3-OMe ligands, whereas chelating dbm anions are found on the remaining coordination sites. The overall topology of the core (Figure 1) is strictly analogous to that of a few hexairon(III)[8] clusters previously studied by our group, as well as that of the hexamanganese(III) complex **1** (Figure 1).[13] A few clusters of divalent transition-metal ions with the same structure, like Zn_7,[22a] Cu_6Na,[22b] Co_6Na,[22c] and Cu_7,[22d] are also known. The structural motif in this class of alkoxide clusters is represented by a closest-packing (c.p.) arrangement of donor oxygen atoms, which recalls the infinite lattices of metal oxides and oxohydroxides.[9a,23,24] Two layers of c.p. oxygen atoms have been often observed in the core of alkoxoiron(III) clusters, with the metal ions arranged in a single planar array.[8,9a,10] More than two layers of oxygen atoms following the abcabc... pattern (cubic closest packing) have been observed in a few instances.[9b,c] In manganese chemistry, this structural motif is apparently less common. Among previously reported examples are mixed-valence $[Mn_7(OH)_3Cl_3(hmp)_9]^{2+}$ (**8**)[12,25] and $[Mn_{10}O_{14}(tren)_6]^{8+}$ (**9**),[5c,12] which contain double layers of donor atoms (O, N, Cl in **8**; O, N in **9**). Due to the presence of oxygen donors only in the coordination sphere of the metal ions, complexes **1** and **2** represent the most accurate models so far obtained for the infinite lattices of layered manganese oxide minerals. Hexamanganese fragments with the same Mn/O topology observed in **1** are part of the bidimensional layers of chalcophanite, a naturally occurring Mn^{IV} oxide which has been formulated as $ZnMn_3O_7 \cdot 3H_2O$ (Figure 4).[26a] Complex **2** can be formally constructed from **1** by replacing the central sodium ion with a manganese ion (Figure 1). The resulting homometallic layer is very similar to that encountered in lithiophorite, $(Li,Al)MnO_2(OH)_2$, which has been formulated as a nonstoichiometric mixed-valence $Mn^{II,IV}$ mineral.[26b]

The crystallographically imposed equivalence between the manganese ions in the $[Mn_6(OMe)_{12}]$ "crown"[27] is the most intriguing feature of the structure. Electroneutrality requires an average oxidation state of $+^{18}/_7$ for the manganese ions in **2**. Assuming that the cluster comprises manganese ions in the valence states +2, +3, and +4, there are three possible stoichiometries, namely $Mn^{II}_3Mn^{III}_4$, $Mn^{II}_4Mn^{III}_2Mn^{IV}$, and $Mn^{II}_5Mn^{IV}_2$. To our knowledge, molecular species comprising di- and tetravalent manganese ions only have never been isolated in the solid state, although a dimeric $Mn^{II}Mn^{IV}$ complex has been proposed as an intermediate in the activity cycle of manganese catalases from spectroscopic data.[28] The presence of manganese ions in three different oxidation states in the same molecule would be very unusual as well. Only three of such compounds have been reported so far: $[Mn_4O_2(tphpn)_2(H_2O)_2(CF_3SO_3)_2]^{3+}$, in which a $Mn^{III}Mn^{IV}$ pair is flanked by two Mn^{II} ions,[12,29a] $[Mn_{12}O_{12}(O_2CEt)_{16}(H_2O)_4]^-$, whose core has a $Mn^{IV}_4Mn^{III}_7Mn^{II}$ stoichiometry,[4f] and $[Mn_{13}O_8(OEt)_6(O_2CPh)_2]$, a molecule with a "supercubane" structure.[29b] In contrast, high-nuclearity mixed-valence $Mn^{II,III}$ complexes are quite common.[4i-l,5a,b,6a,b,25,27] Consequently, the first stoichiometry proposed seems the most probable. Furthermore, it is consistent with the metrical parameters of the core, as discussed hereafter. Mn1 can be reasonably assigned as a Mn^{II} ion on the basis of the Mn1−O1 bond distances [2.180(2) Å] and of its highly symmetric coordination sphere.[30] On the other hand, the Mn2−O distances are moderately anisotropic, ranging from 2.006(2) to 2.185(2) Å, and point to the presence of a partial Mn^{III} character. In particular, the "whirlpool-like" arrangement of the elongation axes O1−Mn2−O4 in the structure is similar to that found in **1** (Figure 1).[13] To support these observations on a quantitative basis, we carried out bond valence sum calculations. The bond valence (or bond strength)[31-33] concept and its relation with bond lengths and oxidation states of cations were first introduced by Pauling.[32a] The bond valence (S_i) for the *i*th metal−ligand bond is given by

$$S_i = \exp[(r_o - r_i)/B]$$

where r_i is the crystallographically determined bond distance and r_o and B are constants tabulated for the different metal ions in the different oxidation states.[31] The oxidation state V of the

(21) These values are close to those expected for a 1:1 salt (see: Geary, W. J. *Coord. Chem. Rev.* **1971**, *7*, 81).

(22) (a) Tesmer, M.; Muller, B.; Vahrenkamp, H. *J. Chem. Soc., Chem. Commun.* **1997**, 721. (b) Blake, A. J.; Gould, R. O.; Milne, P. E. Y.; Winpenny, R. P. *J. Chem. Soc., Chem. Commun.* **1991**, 1453. (c) McConnell, S.; Motevalli, M.; Thornton, P. *Polyhedron* **1995**, *14*, 459. (d) Blake, A. J.; Gould, R. O.; Grant, C. M.; Milne, P. E. Y.; Reed, D.; Winpenny, R. P. *Angew. Chem., Int. Ed. Engl.* **1994**, *33*, 195.

(23) (a) Hyde, B. G.; Andersson, S. *Inorganic Crystal Structures*; John Wiley & Sons: New York, 1989. (b) Wells, A. F. *Structural Inorganic Chemistry*, 5th ed.; Clarendon Press: Oxford, England, 1984.

(24) Powell, A. K.; Heath, S. L.; Gatteschi, D.; Pardi, L.; Sessoli, R.; Spina, G.; Del Giallo, F.; Pieralli, F. *J. Am. Chem. Soc.* **1995**, *117*, 2491.

(25) Bolcar, M. A.; Aubin, M. J.; Folting, K.; Hendrickson, D. N.; Christou, G. *J. Chem. Soc., Chem. Commun.* **1997**, 1485.

(26) (a) Wadsley, A. D. *Acta Crystallogr.* **1955**, *8*, 165. (b) Wadsley, A. D. *Acta Crystallogr.* **1952**, *5*, 676.

(27) Pecoraro, V. L.; Stemmler, A. J.; Gibney, B. R.; Bodwin, J. J.; Wang, H.; Kampf, J. W.; Barwinski, A. *Prog. Inorg. Chem.* **1997**, *45*, 83.

(28) Sakiyama, H.; Okawa, H.; Isobe, R. *J. Chem. Soc., Chem. Commun.* **1993**, 882.

(29) (a) Chan, M.; Armstrong, W. H. *J. Am. Chem. Soc.* **1990**, *112*, 4985. (b) Sun, Z.; Gantzel, P. K.; Hendrickson, D. H. *Inorg. Chem.* **1996**, *35*, 6640.

(30) Drew, M. B.; Harding, C. J.; McKee, V.; Morgan, G. G.; Nelson, J. *J. Chem. Soc., Chem. Commun.* **1995**, 1035.

(31) Brown, I. D.; Altermatt, D. *Acta Crystallogr.* **1985**, *B41*, 244.

(32) (a) Pauling, L. *J. Am. Chem. Soc.* **1929**, *51*, 1010. (b) Donnay, G.; Allmann, R. *Am. Mineral.* **1970**, *55*, 1003. (c) Pyatenko, Y. *Kristallografiya* **1972**, *17*, 773. (d) Brown, I. D.; Shannon, R. D. *Acta Crystallogr.* **1973**, *A29*, 266. (e) Allmann, R.; Donnay, G. *Abstracts of Papers*, 9th General Meeting of the International Mineralogical Association, West Berlin and Regensburg, 1974; p 89. (f) Brown, I. D *J. Solid State Chem.* **1974**, *11*, 214. (g) Allmann, R. *Monatsh. Miner.* **1975**, *106*, 779. (h) Brown, I. D.; Wu, K. K. *Acta Crystallogr.* **1976**, *B32*, 1957. (i) Brown, I. D. *Chem. Soc. Rev.* **1978**, *7*, 359. See also: Brown, I. D. In *Structure and Bonding in Crystals*; O'Keefe, M., Navrotsky, A., Eds.; Academic Press: New York, 1981; Vol. II, p 1.

(33) Thorpe, H. H. *Inorg. Chem.* **1992**, *31*, 1585.

metal ion is determined self-consistently through the equation

$$V = \sum_i S_i$$

where the sum is carried out over all different bonds.[31] This type of analysis proved to be useful in bioinorganic[33] and material chemistry[34] as well as for various manganese mixed-valence clusters.[4f,6a,33] In our case, $V = 2.09(2)$ [1.93(2)] and 2.89(2) [2.66(2)] for Mn1 and Mn2, respectively, assuming a +2 [+3] oxidation state. It can be concluded that Mn1 is essentially a Mn^{II} ion whereas Mn2 has a noninteger oxidation state between +2 and +3. Modeling Mn2 as $^1/_3Mn^{II} + {}^2/_3$-Mn^{III},[33] a value $V = 2.73(3)$ is calculated, which is in nice agreement with that expected (+2.67). To check the possibility that Mn1 could show a thermally activated valence detrapping, a structure determination at 293 K has been performed. Although the overall quality of the structure is rather poor (R1 = 0.084), no change in the space group was observed. Comparison between bond distances and angles at 188 and 293 K clearly indicates that the valence-trapped character of Mn1 is retained at room temperature (see Supporting Information). The observed solid-state structure can now be ascribed either to (a) static disorder effects in the crystal lattice (class I compounds in the Robin-Day classification[35]), (b) thermally activated intramolecular electron transfer (class II[35]), or (c) electron delocalization (class III[35]). It should be noted that mixed-valent manganese compounds usually show a well-resolved valence-trapped structure in the solid state and therefore belong to class I, presumably due to the large distortions associated with the Jahn−Teller Mn^{III} ion. To our knowledge, rare examples of mixed-valence manganese compounds with crystallographically equivalent metal sites in the solid-state have been reported so far, namely $Mn^{III,IV}$ dimers[36] (class I[35]), a $Mn^{II,III,IV}$ tetramer[29] (class I[35]), and a $Mn^{II}_2Mn^{III}$ basic carboxylate[37] (class II[35]). This feature is also found in lithiophorite, where Mn^{II} and Mn^{IV} sites are indistinguishable.[26b] In our case, an analysis of structural parameters does not permit us to distinguish among (a), (b), and (c).[36a] However, the solid-state electronic spectra are typical of Jahn−Teller-distorted Mn^{III} ions.[16b] They point to the presence of localized Mn^{III} ions on the time scale of UV−vis spectroscopy and rule out full electron delocalization (c). ^{1}H NMR experiments in solution provided further hints, as illustrated in the next section.

^{1}H NMR Studies in Solution. ^{1}H NMR spectroscopy in solution turns out to be a useful tool for investigating the properties of Mn^{III} complexes, which usually show well-resolved spectra due to favorable electronic relaxation times.[38] dbm conveys to metal chelates a good solubility in moderately polar organic solvents such as toluene, $CHCl_3$, and CH_2Cl_2. Solution ^{1}H NMR experiments were thus carried out on **2** and, for comparison, on **4** and on the Mn^{II} complex $[Mn(dbm)_2(H_2O)_2]$ (**6**). As previously found in related Fe^{III} complexes, the phenyl protons of dbm ligands are useful magnetic probes.[8c] In particular, at room temperature *m*-Ph and *p*-Ph protons experience moderate paramagnetic shifts and reasonable line widths in both Mn^{II} and Mn^{III} species.

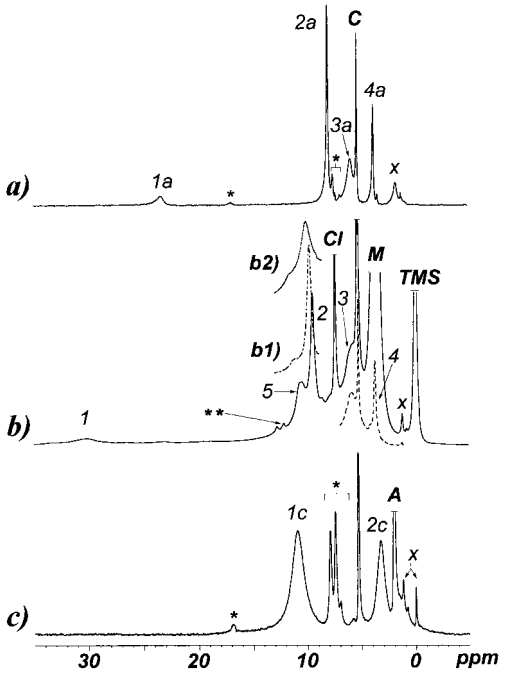

Figure 5. Room-temperature ^{1}H NMR spectra of **4** in CD_2Cl_2 (a), **2** in $CD_2Cl_2-CD_3OD$ (5:1 v/v) (b), **2** in CD_2Cl_2 (b, dashed line, 1−7 ppm region only), and **6** in $CD_2Cl_2-CD_3COCD_3$ (3:1 v/v) (c). Spectra of **2** recorded at 273 K (b_1) and 258 K (b_2) are also shown in the 9−13 ppm region. Peak assignments: (a) 1a = C−H, 2a = *m*-Ph, 3a = *o*-Ph, 4a = *p*-Ph; (b) 1 = C−H (Mn^{III}), 2 = *m*-Ph (Mn^{III}), 3 = *o*-Ph (Mn^{III}), 4 = *p*-Ph (Mn^{III}), 5 = *m*-Ph (Mn^{II}); (c) 1c = *m*-Ph, 2c = *p*-Ph. In addition: Cl = $CHCl_3$, C = $CHDCl_2$, M = CH_3OD; A = CHD_2COCD_3, × = solvent impurities, ∗ = Hdbm [6.87 (C−H), 7.50 (*m*-Ph), 7.56 (*p*-Ph), 8.02 (*o*-Ph), 16.90 (O−H) ppm in $CDCl_3$], ∗∗ = unassigned peaks.

In CD_2Cl_2 solutions of monomeric **4**, four paramagnetically shifted resonances are observed at 23.37 (br, C−H, 1H), 7.97 (*m*-Ph, 4H), 5.94 (br, *o*-Ph, 4H), and 3.80 ppm (*p*-Ph, 2H) (Figure 5a).[39] The assignments have been based on peak area ratios and relative line widths. In particular, since the latter are inversely related to the distance of the proton from a paramagnetic center,[38] the peak at 5.94 ppm can be assigned to *o*-Ph protons with confidence. Due to the anisotropic nature of the magnetic susceptibility tensor in Mn^{III} complexes, both contact and pseudocontact effects are expected to contribute to the observed shifts. Detailed HF-EPR studies on **4** in the solid state recently showed that the ground spin-quintet term of Mn^{III} is largely split in zero magnetic field with $D = -4.35$ cm^{-1} and $E = 0.26$ cm^{-1}.[1a,16b] Pseudocontact shifts for the protons in **4** were then evaluated from structural data and spin-Hamiltonian parameters.[38] Absolute shifts smaller than 0.25 ppm were obtained, indicating that the observed paramagnetic shifts are essentially contact in nature. This conclusion was confirmed by the temperature dependence of the observed shifts,

(34) Brown, I. D. *Solid State Chem*. **1989**, *82*, 122.
(35) Robin, M. B.; Day, P. *Adv. Inorg. Chem. Radiochem*. **1967**, *10*, 247.
(36) (a) Stebler, M.; Ludi, A.; Burgi, H.-B. *Inorg. Chem.* **1986**, *25*, 4743. (b) Wieghardt, K.; Bossek, U.; Zsolnai, L.; Huttner, G.; Blondin, G.; Girerd, J.-J.; Babonneau, F. *J. Chem. Soc., Chem. Commun.* **1987**, 651. (c) Goodson, P. A.; Hodgson, D. J.; Michelsen, K. *Inorg. Chim. Acta* **1990**, *172*, 49. (d) Goodson, P. A.; Hodgson, D. J.; Glerup, J.; Michelsen, K.; Weihe, H. *Inorg. Chim. Acta* **1992**, *197*, 141.
(37) (a) Vincent, J. B.; Chang, H.-R.; Folting, K.; Huffmann, J. C.; Christou, G.; Hendrickson, D. N. *J. Am. Chem. Soc*. **1987**, *109*, 5703. (b) Jang, H. G.; Vincent, J. B.; Nakano, M.; Huffmann, J. C.; Christou, G.; Sorai, M.; Wittebort, R. J.; Hendrickson, D. N. *J. Am. Chem. Soc*. **1989**, *111*, 7778. (c) Meesuk, L.; White, R. P.; Templeton, B.; Jayasooriya, U. A.; Cannon, R. D. *Inorg. Chem.* **1990**, *29*, 2389.
(38) Bertini, I.; Luchinat, C. *Coord. Chem. Rev.* **1996**, *150*, 1.
(39) Unassigned ^{1}H NMR spectra of **4** were reported by: Kissler, K. D.; Sheppard, S. K.; Eaton, G. R.; Eaton, S. S. *J. Magn. Reson.* **1985**, *63*, 74. The phenyl protons of benzoate ligands coordinated to Mn^{III} give rise to very similar resonances (see: Wemple, M. W.; Tsai, H.-L.; Folting, K.; Hendrickson, D. N.; Christou, G. *Inorg. Chem.* **1993**, *32*, 2025).

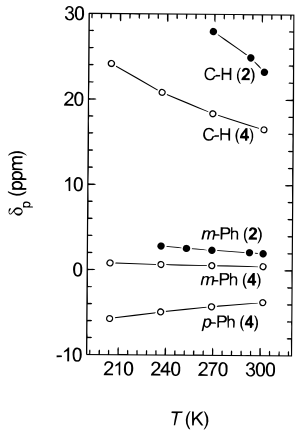

Figure 6. Paramagnetic shift vs *T* plots for the different protons in **2** and **4**. The paramagnetic shift for the *i*th proton is defined as $\delta_p(i) = \delta(i) - \delta_{Hdbm}(i)$ where $\delta(i)$ is the observed chemical shift and $\delta_{Hdbm}(i)$ is the chemical shift in free Hdbm.

which follow a Curie−Weiss law in the range 213−303 K (Figure 6).

The ^{1}H NMR spectrum of **2** in $CDCl_3$ shows a large number of peaks in the 0−15 ppm region, pointing to substantial dissociation of the cluster. As previously found for related complexes,[7a] methanol has a stabilizing effect, and much simpler spectra are reproducibly obtained in CD_2Cl_2−CD_3OD and $CDCl_3$−CD_3OD mixtures. In CD_2Cl_2−CD_3OD 5:1 (v/v), the room-temperature spectrum is dominated in the 5−50 ppm region by a narrow resonance at 9.47 ppm while broad bands appear at 5.72 and 30.12 ppm (Figure 5b). The spectrum in CD_2Cl_2 shows an additional narrow resonance at 3.56 ppm (Figure 5b, dashed line) which is most probably obscured by the strong peak from methanol-d_1 at 3.52 ppm (vide infra). The overall pattern of resonances so far described is consistent with that expected for a set of localized [Mn^{III}(dbm)] units. The ^{1}H NMR spectrum of **6** (Figure 5c) allowed us to complete our analysis. The set of sharp peaks present between 6 and 9 ppm can be ascribed to the presence of free Hdbm in solution and point to a partial dissociation of the complex while the paramagnetically broadened signals found at 3.24 (br, 1H) and 10.95 (br, 2H) ppm have been assigned to *p*-Ph and *m*-Ph protons, respectively, from peak area ratios and by comparison with the spectra Fe^{III}(dbm) complexes.[8c] On this basis, the broad resonance at 10.7 ppm for **2** is assigned to [Mn^{II}(dbm)] units. The observation of distinct resonances for Mn^{II} and Mn^{III} sites proves that valence is trapped on the NMR time scale. Compelling evidence that the solid-state structure is most probably retained in solution comes from the strong signal at 3.52 ppm, which is typical of CH_3-type protons and is not observed unless CD_3OD is added to the solution. This indicates that a strong magnetic interaction exists between the metal centers and the protons of methoxide ligands,[7a] which becomes detectable after the fast-exchange reaction

$$Mn{-}OCH_3 + CD_3OD \rightarrow Mn{-}OCD_3 + CH_3OD$$

The temperature dependence of the spectrum was found to be consistent with the solid-state magnetism of **2**. Upon lowering of the temperature, the signals of *m*-Ph and C−H protons broaden dramatically while shifting downfield (Figure $5b_{1-2}$) and become undetectable below 240 K. Assuming dominant contact contributions to the paramagnetic shifts in **2** as in **4**, the temperature dependence of paramagnetic shifts points to an increased unpaired-spin density on the metal centers at low temperature as compared to the case of **4** (Figure 6). This qualitatively matches the smooth increase of χT observed in the solid state.

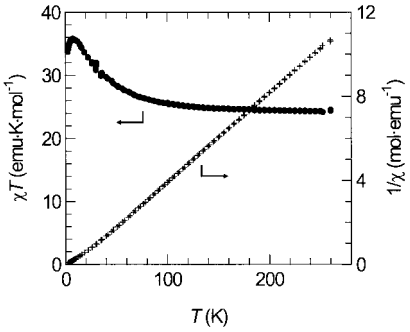

Figure 7. Experimental χT vs *T* and $1/\chi$ vs *T* plots for **2**.

Magnetic Studies. The magnetic susceptibility of **3** follows a Curie−Weiss law down to 20 K with $C = 5.95$ emu K mol^{-1} and $\Theta = -2.00$ K. The *C* value agrees well with two Mn^{III} ions ($C = 6.00$ emu K mol^{-1} for $g = 2.00$). Experimental data were quantitatively analyzed, including single-ion magnetic anisotropies, Zeeman interactions, and isotropic exchange coupling between the two high-spin Mn^{III} ions ($S = 2$). Single-ion anisotropy tensors were assumed to be axial, and collinear as required by the solid-state structure. A least-squares fit of magnetic data, based on full diagonalization of the spin Hamiltonian, resulted in two sets of best-fit parameters: (a) $D = -2.5(4)$ cm^{-1}, $J = 0.28(4)$ cm^{-1}, $g = 1.983(2)$; (b) $D = 8.7(2)$ cm^{-1}, $J = -0.24(4)$ cm^{-1}, $g = 1.971(2)$. Although the second set led to a slightly better agreement with experimental data, its physical significance is questionable due to the large and positive *D* parameter. Set (a) appears to be more realistic for tetragonally elongated Mn^{III} complexes, which usually have $D < 0$.[16b] In any case, the reported *J* values are much smaller than that found for the isostructural Fe^{III} dimer **7**[10] and well illustrate the effect of removing one 3d electron when passing from high-spin Fe^{III} ($3d^5$) to high-spin Mn^{III} ($3d^4$). However, the actual sign of *J* in magnetically coupled Mn^{III}_2 units depends on the relative orientation between Jahn−Teller axes and on the subtle balance between different exchange pathways, as predicted by Goodenough and Kanamori[40] and extensively discussed by Wieghardt et al.[41] When the Mn−O−Mn moiety comprises one axial and one equatorial bond,[42] as found in **3**, weak antiferromagnetic couplings are usually observed.[42a−d] This indicates that the expected ferromagnetic contribution from "crossed" exchange pathways involving half-filled orbitals on one metal and empty orbitals on the other metal (e.g., $d_{x^2-y^2}$−d_{z^2}) is offset by antiferromagnetic pathways involving one half-filled orbital on each metal center.[1a,40,41]

The solid-state magnetic behavior of **2** has been studied in detail. A χT vs *T* plot obtained with an applied field of 1 kG for $2.2 < T < 30$ K and 10 kG for $30 < T < 260$ K is reported in Figure 7. χ strictly follows a Curie−Weiss law in the temperature range 40−260 K, with $C = 23.47$ emu K mol^{-1} and $\Theta = 8.15$ K. The value of the *C* constant is closer to that

(40) Ginsberg, A. *Inorg. Chim. Acta Rev.* **1971**, *5*, 45 and references therein.
(41) Hotzelmann, R.; Wieghardt, K.; Flörke, U.; Haupt, H.-J.; Weatherburn, D. C.; Bonvoisin, J.; Blondin, G.; Girerd, J.-J. *J. Am. Chem. Soc.* **1992**, *114*, 1681.
(42) (a) Yu, S.-B.; Wang, C.-P.; Day, E. P.; Holm, R. H. *Inorg. Chem.* **1991**, *30*, 4067. (b) Matsumoto, N.; Zhong, Z. J.; Okawa, H.; Kida, S. *Inorg. Chim. Acta* **1989**, *160*, 153. (c) Vincent, J. B.; Folting, K.; Huffman, J. C.; Christou, G. *Inorg. Chem.* **1986**, *25*, 996. (d) Kennedy, B. J.; Murray, K. S. *Inorg. Chem.* **1985**, *24*, 1552. (e) Gelasco, A.; Pecoraro, V. L. *J. Am. Chem. Soc.* **1993**, *115*, 7928.

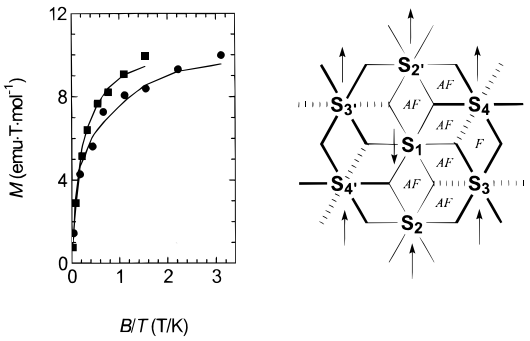

Figure 8. (a) Experimental M vs B/T data for **2** at 2.2 K (●) and 4.6 K (■) and best-fit calculated curves for $S = {}^{17}/_{2}$ with the parameters given in the text. (b) Possible C_i-symmetry arrangement of the Mn^{II} (S_1, S_2, $S_{2'}$) and Mn^{III} (S_3, S_4, $S_{3'}$, $S_{4'}$) ions in **2**; equatorial and axial $Mn^{III}-O$ bonds are represented by bold and broken lines, respectively. The expected sign of each pairwise exchange interaction is also indicated (AF = antiferromagnetic; F = ferromagnetic).

expected for the $Mn^{II}_3Mn^{III}_4$ formulation (25.13 emu K mol^{-1} with $g = 2.00$) than for the alternative stoichiometries $Mn^{II}_4Mn^{III}_2Mn^{IV}$ and $Mn^{II}_5Mn^{IV}_2$ (25.38 and 25.63 emu K mol^{-1}, respectively). The smooth increase of χT on lowering the temperature points to a tendency of the spin vectors to align in a parallel fashion. The spin ground state of the cluster, which contains an odd number of unpaired electrons, can take any half-integer value between $^1/_2$ and $^{31}/_2$. Comparison of the low-temperature χT values with those expected for the different values of S (31.9 emu K mol^{-1} for $S = {}^{15}/_{2}$; 40.4 emu K mol^{-1} for $S = {}^{17}/_{2}$; 49.9 emu K mol^{-1} for $S = {}^{19}/_{2}$) gives some indication of an $S = {}^{17}/_{2}$ ground state. Magnetization curves recorded at 2.2 and 4.6 K for fields up to 70 kG revealed no tendency to reach saturation and were analyzed assuming an isolated zero-field-split ground multiplet.[4e−g,i] Least-squares fits of experimental data gave (a) $g = 2.36(6)$ and $D = -0.34(6)$ cm^{-1} for $S = {}^{15}/_{2}$, (b) $g = 2.08(5)$ and $D = -0.27(5)$ cm^{-1} for $S = {}^{17}/_{2}$ (Figure 8a), (c) $g = 1.86(5)$ and $D = -0.21(4)$ cm^{-1} for $S = {}^{19}/_{2}$. While the best-fit g factor obtained for $S = {}^{15}/_{2}$ is unacceptably high for a complex containing Mn^{II} and Mn^{III} ions only, reasonable sets of parameters result from $S = {}^{17}/_{2}$ and $^{19}/_{2}$, thus confirming our analysis of χT vs T data. It should be noted, however, that the suggested assignment of Mn1 as a Mn^{II} ion leads to three possible arrangements of the remaining Mn^{II} centers in positions 1−2, 1−3, and 1−4, respectively, of the external "crown". Since it is not possible to establish a priori the actual contribution of each arrangement to the observed magnetic behavior, $S = {}^{17}/_{2}$ must be taken as a lower limit to the S value of one of the three possible topologies.[24] As recently pointed out Hendrickson et al., the quantitative analysis of magnetic data is further complicated by the fact that $Mn^{II}-Mn^{II}$, $Mn^{II}-Mn^{III}$, and $Mn^{III}-Mn^{III}$ exchange interactions through alkoxide bridges should have comparable magnitudes.[25] Spin frustration effects may therefore play an important role, and the spin multiplicity of the ground state can easily escape prediction. In addition, high-spin Mn^{III} ions are susceptible of Jahn−Teller distortion. Superexchange interactions are strongly influenced by the orientation of the Jahn−Teller axes,[1a,41] and a large number of different pairwise interactions is therefore expected. The origin of spin frustration can be illustrated by considering the simplest case of a centrosymmetric core. In principle, six different exchange-coupling constants J_{ij} can be envisaged between nearest neighbors (Figure 8b). However, some simplification may be introduced by setting $J_{13} = J_{14}$ since they are both $Mn^{III}(ax+eq)-Mn^{II}$ interactions. If the relations $J_{34} < 0$ and J_{12}, J_{13}, J_{23}, $J_{14} > 0$ hold,[40,41] spin frustration is expected within the triangular arrays 1−2−3 and 1−2′−4 (see caption to Figure 8).

Conclusions

The use of alkoxide ligands represents a convenient strategy for assembling high-nuclearity manganese clusters. In particular, simultaneous aggregation and oxidation of Mn^{II} ions are efficient routes to $Mn^{II,III}$ polynuclear complexes. As found for alkoxoiron(III) clusters, the metal/oxygen core is invariably based on a closest-packing arrangement of oxygen atoms which structurally recalls layered metal oxides. The cation $[NaMn^{III}_6(OMe)_{12}(dbm)_6]^+$ in **1**[13] has the same basic structure as the mineral chalcophanite, whereas $[Mn_7(OMe)_{12}(dbm)_6]$ (**2**) closely resembles lithiophorite and can be formally constructed from **1** by replacing the central sodium ion with a manganese ion. Complex **2** is a mixed-valence species containing three Mn^{II} and four Mn^{III} ions. Although solid-state structural data at 188 K point to 6-fold molecular symmetry, ^{1}H NMR experiments in solution indicate that valence is trapped on the NMR time scale (class I[35]). The electronic ground states of both **1** and **2** are characterized by remarkably large spin multiplicities. The Mn^{III} ions in **1** are ferromagnetically coupled through μ_2-OMe ligands to give an $S = 12$ ground state.[13] Magnetic data for **2** are consistent with an $S = {}^{17}/_{2}$ ground state. Due to their direct structural resemblance to bulk manganese oxides, complexes **1** and **2** represent unique additions to the growing pool of high-spin magnetic clusters so far reported.

Acknowledgment. We thank Prof. S. J. Lippard and Dr. P. Fuhrmann (MIT, Cambridge, MA) for providing low-temperature X-ray data for **2**. The financial support of the Italian MURST and CNR is gratefully acknowledged.

Supporting Information Available: Listings of molar magnetic susceptibility vs temperature and magnetization vs field data and tables of selected interatomic distances and angles for **2** at 188 and 293 K (4 pages). Three X-ray crystallographic files, in CIF format, for **2** (at 188 and 293 K) and **3** are available on the Internet only. Ordering and access information is given on any current masthead page.

IC9800029